Enhancing Wireless Communication Privacy with Artificial Fading

Ting Wang and Yaling Yang
Department of Electrical and Computer Engineering
Virginia Polytechnic Institute and State University
Email: {wangting, yyang8}@vt.edu

***Abstract*—This paper addresses the problem of anti-eavesdropping in wireless network physical layer. The main contribution of this paper is twofold. First, we propose a novel concept of *artificial fading* that is produced by double-beam switching of smart antenna array to intentionally corrupt unwanted wireless communication links. Second, we develop a physical layer anti-eavesdropping scheme to minimize the unnecessary coverage area, and hence, lower the chance of being eavesdropped. Our anti-eavesdropping scheme employs smart antenna with two synthesized radiation patterns, which are optimized to provide good signal quality to the intended receiver, while their overlap apart from the intended direction is minimized. During the transmission, the transmitter periodically alternates between the two optimized patterns at a high frequency, which produces severe fading to the received signal in undesired directions. Since such signals are corrupted and cannot be decoded, eavesdropping is prevented. Simulation experiments show that our anti-eavesdropping scheme outperforms single pattern beamforming in reducing the unnecessary coverage area exposed to eavesdroppers.**

I. Introduction

With the advances in wireless data networking, the amount of confidential information communicated through "free medium" is greater than ever. However, leaving those important data floating in the space is dangerous and vulnerable to eavesdropping attack.

Generally, there are two complementary types of schemes to combat eavesdropping attack. The first type includes cryptographic techniques which are based on the premise that deciphering without knowledge of the secret key is computationally infeasible [1]. The second type is physical layer security schemes that aim at hiding the protected radio signal to the passive eavesdroppers. In this paper, we focus on the latter.

Physical layer security schemes are usually following two concepts: intentionally adding interference to the eavesdropping channels or reducing the coverage region of the transmitter. To generate interference to the eavesdropping channels, the authors in [2] and [3] use antenna array redundancy to create random interference to the eavesdropping channel, while in [4] and [5], artificial noise is introduced to confuse the eavesdropper with carefully designed noise signals which can be canceled at the intended receiver. These schemes require that the channel response from the transmitter to the receiver is perfectly estimated and known to the transmitter. This is realized by either assuming that the communication channel is reciprocal or the transmitter gets feed back about the channel information from the receiver. On the other hand, methods that reduce coverage region lower the chances of eavesdropping by stopping the eavesdroppers from hearing the transmitted signal. In [6] and [7], the authors propose to use collaboration of multiple Access Points (APs) equipped with smart antenna arrays to reduce the region exposed to eavesdroppers. These schemes modify the network protocol to segment the original network packets into fragments. These fragments then are sent by different APs. These schemes are only applicable to network infrastructures with high density of APs.

In this paper, we present a novel physical layer security strategy named "artificial fading" to reduce the coverage region of a transmitter. We employ smart antenna array at the sender to periodically switch the radiation pattern between a pair of predesigned beamforming patterns at a high frequency. These two patterns are designed to both have high constant directional gain towards the intended receiver. However, in all the other directions, the overlapping area between them is minimized. In this way, the double-beam switching process intentionally creates a fast fading effect, named artificial fading, to severely degenerate the signal in the unintended directions and hence reduce the unnecessary coverage. Therefore, there is little space where an eavesdropper can get the signal and, hence, the transmitted information is protected. The detailed contributions of our work are as follows:

- We present the novel concept of artificial fading to support physical layer anti-eavesdropping.
- We propose the method for designing optimal switched beamforming patterns to generate artificial fading.
- We provide insightful evaluation of the performance of the proposed artificial fading scheme.

Comparing to existing approaches, artificial fading has the following benefits: *First, it does not require special deployment of the network infrastructures; Second, it does not require collaboration from other nodes in the network.* Our work shows that when single pattern beamforming scheme already reaches the optimum of minimizing unnecessary coverage area, we are still able to further reduce the unnecessary coverage area using artificial fading.

The rest of the paper is organized as follows. The backgrounds about terminologies, threat model and smart antenna

are introduced in Section II. Section III describes the proposed scheme, artificial fading, and analyze its effectiveness for anti-eavesdropping. The modeling of antenna pattern optimization is presented in section IV. Experimental results are reported in Section V. Section VI discusses and Section VII concludes the paper.

II. Background

In this section we present the important definitions used throughout this paper and introduce the threat model of eavesdropping attacks.

A. Definitions of different signal coverages

Generally, the "coverage area" can be understood as the locations where the radiated signal can be heard, or, the area within which a wireless network user can successfully use the network service. However, the coverage areas can be classified into various levels which require different signal qualities. Thus, to be specific, we present the definitions of coverage areas under different signal quality requirements and use different names to differentiate them throughout this paper.

1) Effective coverage: The region within which the signal quality is good enough for successful decoding of the transmitted signal.

2) Invalid coverage: The region where the existence of the transmitted signal can be detected but the signal quality is not good enough for decoding the signal.

3) Unnecessary coverage: The region apart from the target receiver within the effective coverage area. It has little contribution to the wireless link between the transmitter and the receiver. However, it brings the risk of eavesdropping. Our proposed scheme aims at reducing this unnecessary coverage area, and hence, lowers the chance of being eavesdropped.

B. Eavesdropping threat model

We assume that a communication link is set up between a pair of legitimate nodes. Packets carrying confidential information are broadcasted over the air. As an example illustrated in Fig. 1, the effective coverage region of the transmitter is represented by the shaded area. A node, either the receiver or an adversarial eavesdropper, can receive the packets as long as it is located within the effective coverage of the transmitted signal. Thus an eavesdropper within the effective coverage can silently sniff the transmitted packets. Even if the leaked packets are encrypted, the eavesdropper may take effort to crack the encryption to extract the original data, or do data mining to obtain valuable information.

As we can see, the larger the effective coverage, the higher the risk of eavesdropping. Thus in this paper, the objective of our strategy is to reduce the unnecessary coverage apart from the direction to the receiver.

C. Smart antenna beamforming

A smart antenna array consists of multiple antenna elements. The geometric arrangement of the antenna elements varies according to different designs. However, the common idea of

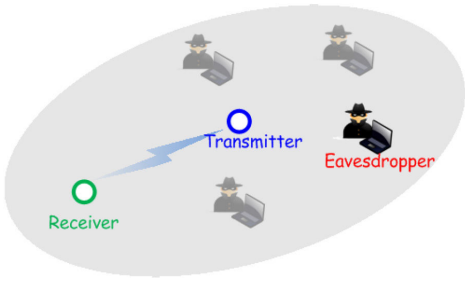

Fig. 1. Eavesdropping threat.

smart antenna arrays is that the amplitudes and phases of the current excitations to the antenna elements are controlled to obtain a desired synthesized radiation pattern. Mathematically, the current excitations are modeled as a complex weight vector. The process of adjusting the complex weight vector to synthesize a desired pattern is called beamforming [8]. Traditionally, beamforming is considered more suitable to be implemented at the APs or base stations in wireless networks. However, recent studies show that beamforming can also be realized on mobile devices [9], [10].

A fully adaptive smart antenna array has both static and dynamic capabilities of beamforming. The static beamforming capability is the ability to produce a specific pattern that satisfies the application requirement, such as minimizing the side lobe level when given a fixed main beam width, and vice versa. On the other hand, the dynamic capability means that the smart antenna is able to vary the synthesized pattern dynamically to meet the changing requirement. One metric for the dynamic performance of smart antennas is the transition time between two radiation patterns. Currently, advanced smart antenna products are able to switch beam patterns in sub-microsecond given the predefined beamforming patterns [11]. Some of them can even finish the pattern re-configuration in tens of nanoseconds [6]. Thus using the advanced smart antenna hardware, the operation of our artificial fading scheme can be fulfilled within a very short period.

III. Artificial Fading

This section provides detailed introduction to the effectiveness of artificial fading.

A. Concept

Traditional beamforming based anti-eavesdropping methods based on smart antenna reduce the unnecessary coverage by simply reducing the transmit power to unintended directions, whereas the suppression capability is quite limited, especially for antenna array with fewer elements. This bottleneck is caused by the tradeoff between the side lobe level and the main beam width of a synthesized beamforming pattern, which means that if we want to decrease either the side lobe level or the main beam width, we have to increase the other. To break this bottleneck, we employ a smart antenna array at the transmitter end to produce two switched beamforming patterns. These two beamforming patterns are designed to satisfy

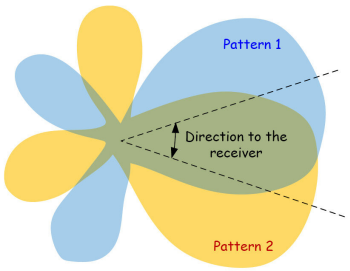

Fig. 2. Illustration of a pattern pair for beam switching.

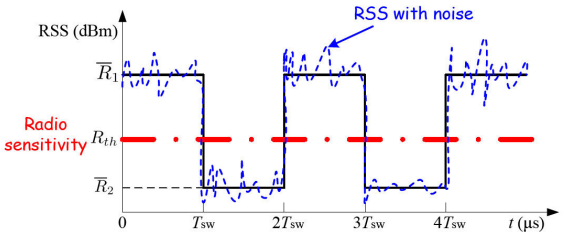

Fig. 3. RSS fluctuation under artificial fading.

two requirements. First, in the direction to the receiver, they both have persistent high directional gain to ensure good signal quality to the receiver. Second, in all the other directions, the overlap between these two patterns is minimized, meaning that the high gain directions of one beamforming pattern correspond to the null directions of the other beamforming pattern. Fig. 2 is a simple illustration of the described pattern pair. During the transmission, the smart antenna array alternates between these two patterns at a high frequency. As a result, the receiver is getting persistent high quality signal, while in other directions, the RSS is changing dramatically and only incomplete frame fractions can be detected, which cannot be used to successfully recover the original signal. This periodical severe variation of the signal strength acts similarly to signal fading in wireless communication channels. Thus we name such signal variation intentionally produced by beam switching of smart antenna as "***Artificial Fading***". The locations where only incomplete frame fractions can be received are actually within the invalid coverage region. We will show that by means of artificial fading, we are able to produce larger reduction of unnecessary coverage comparing to single beamforming pattern.

B. Feasibility

In physical layer data transmissions, signal outage happens when deep fading causes the RSS falling below the radio sensitivity level. Burst of bit errors occurs during the signal outage period. When the bit error rate goes beyond the capability of the error correction code, the whole frame is corrupted. The role of artificial fading is to create high-frequency periodical signal outage to the unintended transmit directions. To this end, we define the switching period as T_{sw}, which is set to be half of the physical layer data frame duration. State-of-the-art smart antennas can perform beam switching in less than one microsecond [6] [11]. Thus, as long as the transition time of beam switching is negligible compared with the frame duration, it is feasible to carry out artificial fading during signal transmission.

To analyze the effectiveness of artificial fading, we use WLAN as an example. The minimum Physical Layer Convergence Protocol (PLCP) frame duration in WLANs is from tens of microseconds to more than 100 microseconds. Thus, a beam switching transition time less than one microsecond is negligible compared with the PLCP frame duration. Suppose at a specific location around the transmitter, while the path losses to the location are the same for two beamforming patterns 1 and 2, the antenna directional gains of these two patterns are different, which results in different average RSSs, denoted as $\overline{R}_1$ and $\overline{R}_2$ for these two patterns. Fig. 3 shows how the signal strength fluctuates at this location when the two patterns are switched. When either $\overline{R}_1$ or $\overline{R}_2$ is lower than the radio sensitivity threshold, signal outage happens periodically at this location and causes bursts of bit errors. Next, we will show that such signal outage is beyond the tolerance of the error correction algorithm used in WLANs.

The error correction capability of an error correction code is defined as the number of bit errors (t_{ecc}) within a code word that can be corrected. For convolutional code, t_{ecc} is bounded by the free distance (d_{free}) following the relationship [12]

$$t_{ecc} = \lfloor \frac{d_{free} - 1}{2} \rfloor. \tag{1}$$

IEEE 802.11 standards use $K = 7$ convolutional code with a minimum code rate $\frac{1}{2}$ [13]. Higher code rate can be achieved by puncturing the "basic" rate $\frac{1}{2}$ code. Additionally, interleaving is used to avoid burst bit errors. Thus, we can consider that the bit errors caused by signal outage are randomly scattered across the whole frame. The largest d_{free} of $K = 7$ convolutional code is 10, which is reached under code rate $\frac{1}{2}$ by adding 7 redundant bits to the 7 information bits. So a code word of $K = 7$ rate $\frac{1}{2}$ convolutional code contains totally 14 bits. By plugging in $d_{free} = 10$ into equation (1), we can get that the 14 bits convolutional code word is able to correct up to 4 bit errors. In other words, the $K = 7$ convolutional code does not work when the bit error rate goes higher than $\frac{5}{14}$. While under the intentioned artificial fading, the signal outage probability is approximately $\frac{1}{2}$, which is out of the error correction capability of $K = 7$ convolutional code. Thus, we are safe to say that at a specific location, as long as the RSS under one of the two switched beamforming patterns is below the radio sensitivity threshold, no PLCP frame can be correctly decoded, and hence, this location is under invalid coverage.

It is worth mentioning that our artificial fading scheme is not limited to WLAN networks. It can also be applied to other wireless networks as long as the transition time between the switched beamforming pattern is much less than the duration of the physical layer data frame and the signal outage produced by artificial fading is beyond the error correction capability of the coding scheme used by the wireless network protocol.

As a result of the proposed artificial fading scheme, the effective coverage area of the transmitter only includes the locations where under both of the two switched beamforming pattern, the RSS is higher than the radio sensitivity. In the following sections, we use this conclusion to calculate the effective coverage area of double-beam switching transmission.

IV. Minimization of Unnecessary Coverage

In this section, we first describe the prediction of effective coverage area under our artificial fading scheme. Then we formulate the problem of minimizing unnecessary coverage based on the mathematical relationship between the antenna array weight vector and the effective coverage area.

A. Smart antenna model

In the remainder of this paper, we assume that the radio station is equipped with a circular smart antenna array, which consists of N_{ant} isotropic elements placed over a circle with radius R. The i^{th} antenna element is located with the phase angle ϕ_i. The beamforming pattern of this circular smart antenna array is expressed as below [14]

$$G(\theta) = \sum_{i=1}^{N_{ant}} w_i \exp[j\frac{2\pi}{\lambda} R\cos(\theta - \phi_i)], \tag{2}$$

where λ is the signal wavelength, θ represents the direction and $\mathbf{w} = [w_1, w_2, \cdots w_{N_{ant}}]^H$ is the complex weight vector that can be tuned to change the radiation pattern.

We choose circular antenna array as an example to illustrate the design of our scheme because it can produce flexible asymmetric beamforming patterns and easily deflect a beam through 2π [8]. However, it is important to note that our scheme also works with antennas with other geometric forms, such like planar arrays. Although their beamforming functions differ from equation (2), since their radiation patterns are also determined by the complex weight vectors, they can still work with our scheme by simply replacing equation (2) with their corresponding beamforming functions.

B. Prediction of effective coverage area

In order to minimize the unnecessary coverage area of the transmitted signal, we use log-distance path loss model to predict the mean RSSs at given distances and calculate the predicted effective coverage area. Although the practical wireless communication channels can be more complicated and the real coverage area is extremely hard to predict, we believe that the log-distance path loss model is effective in providing predictions and guidance in an average sense and is the best option when accurate channel condition information cannot be obtained.

1) Effective coverage area of single pattern beamforming: According to the log-distance path loss model, the mean path loss at distance d is given by

$$\overline{PL}(d)(\text{dB}) = 10\alpha\log_{10} d + PL_0(\text{dB}), \tag{3}$$

where PL_0 is the path loss at the reference distance $d_0 =$ 1 m, α is the path loss exponent and d is the distance from the transmitter to the interested location. In order to calculate the signal coverage area, we let r be the distance from the transmitter to the location where the signal strength is the radio sensitivity threshold. Hence we have

$$\overline{PL}(r)(\text{dB}) = P_0(\text{dBm}) - R_{th}(\text{dBm}). \tag{4}$$

Here P_0 is the required transmit power to keep good connection with the receiver if omnidirectional antenna is used. R_{th} denotes the radio sensitivity threshold. By combining (3) and (4), we get

$$10\alpha\log_{10} r = P_0(\text{dBm}) - PL_0(\text{dB}) - R_{th}(\text{dBm}), \tag{5}$$

$$r = \left(\frac{P_0}{R_{th} PL_0}\right)^{\frac{1}{\alpha}}. \tag{6}$$

For smart antenna, the radiation power at direction θ is also determined by the directional gain $|G(\theta)|^2$ in addition to P_0. So we rewrite equation (6) as

$$r(\theta) = \left(\frac{P_0|G(\theta)|^2}{R_{th} PL_0}\right)^{\frac{1}{\alpha}}. \tag{7}$$

According to the area integral formula in polar coordinates, the predicted effective coverage area A is calculated by

$$\begin{aligned} A &= \tfrac{1}{2}\int_0^{2\pi} r^2(\theta)\,\mathrm{d}\theta \\ &= \tfrac{1}{2}\int_0^{2\pi} \left(\tfrac{P_0|G(\theta)|^2}{R_{th} PL_0}\right)^{\frac{2}{\alpha}}\,\mathrm{d}\theta \\ &= \tfrac{1}{2}\left(\tfrac{P_0}{R_{th} PL_0}\right)^{\frac{2}{\alpha}} \int_0^{2\pi} |G(\theta)|^{\frac{4}{\alpha}}\,\mathrm{d}\theta. \end{aligned} \tag{8}$$

If we uniformly divide the space $[0, 2\pi)$ into M small sectors, we are able to transform equation (8) into discret form.

$$A \approx \frac{\pi}{M}\left(\frac{P_0}{R_{th} PL_0}\right)^{\frac{2}{\alpha}} \sum_{m=0}^{M-1} |G(\theta_m)|^{\frac{4}{\alpha}},\ \theta_m = \frac{2\pi m}{M}. \tag{9}$$

2) Effective coverage area under double-beam switching: Because a pair of radiation patterns are employed in the proposed anti-eavesdropping scheme, we use a superscript to differentiate the patterns. Thus, according to (2), the n^{th} beamforming pattern is determined by the complex weight vector $\mathbf{w}^{(n)}$ and the beamforming pattern is given by

$$\begin{aligned} &G^{(n)}(\theta) = \sum_{i=1}^{N_{ant}} w_i^{(n)} \exp[j\tfrac{2\pi}{\lambda} R\cos(\theta - \phi_i)], \\ &n = 1, 2. \end{aligned} \tag{10}$$

Therefor, the effective coverage radius of the n^{th} beamforming patterns is

$$r^{(n)}(\theta) = \left(\frac{P_0|G^{(n)}(\theta)|^2}{R_{th} PL_0}\right)^{\frac{1}{\alpha}},\ n = 1, 2. \tag{11}$$

As shown in Section III, a wireless communication link is unusable when its RSS under at least one of the two beamforming patterns is lower than the radio sensitivity level.

Thereby, we define the effective coverage radius under double-beam switching as

$$r_{sw}(\theta) = min\{r^{(1)}(\theta), r^{(2)}(\theta)\}. \tag{12}$$

Thus, the effective coverage area of double-beam switching transmission is described by

$$A_{sw} = \frac{1}{2}\int_0^{2\pi} r_{sw}^2(\theta)\,\mathrm{d}\theta. \tag{13}$$

By dividing the space $[0, 2\pi)$ into M small sectors, A_{sw} can be approximately expressed as:

$$\begin{aligned} &A_{sw} \approx \tfrac{\pi}{M}\left(\tfrac{P_0}{R_{th}PL_0}\right)^{\frac{2}{\alpha}} \sum_{m=0}^{M-1} |G_{sw}(\theta_m)|^{\frac{4}{\alpha}}, \\ &|G_{sw}(\theta_m)| = min\{|G^{(1)}(\theta_m)|, |G^{(2)}(\theta_m)|\}, \\ &\theta_m = \tfrac{2\pi m}{M}. \end{aligned} \tag{14}$$

C. Double-pattern optimization

Since the signal towards the intended receiver should have a high quality, we assume that the main beam of the two beamforming patterns should overlap for at least a certain width in the direction to the intended receiver. This beamwidth of the overlapped main beams is defined as BW. The effective coverage outside BW is unnecessary coverage since it has little contribution to quality of the intended communications, while it provides space for hidden eavesdroppers.

Assuming the receiver's direction is $\theta = 0°$, the desired main beam region is $[-\frac{BW}{2}, \frac{BW}{2}]$ and directions outside this region are unwanted transmit directions which cause unnecessary coverage. In order to simplify the formulas in discrete form, we define $\Delta = \frac{2\pi}{M}$, which represents the size of every discrete sector. Letting

$$l = \lfloor \frac{BW}{2\Delta} \rfloor, \tag{15}$$

the unnecessary coverage area for single beamforming pattern can be derived from (9) as:

$$U \approx \frac{\pi}{M}\left(\frac{P_0}{R_{th}PL_0}\right)^{\frac{2}{\alpha}} \sum_{m=l}^{M-1-l} |G(\theta_m)|^{\frac{4}{\alpha}},\ \theta_m = m\Delta. \tag{16}$$

For the artificial fading scheme, according to (14), the unnecessary coverage area of double-beam switching transmission can be expressed as:

$$\begin{aligned} &U_{sw} \approx \tfrac{\pi}{M}\left(\tfrac{P_0}{R_{th}PL_0}\right)^{\frac{2}{\alpha}} \sum_{m=l}^{M-1-l} |G_{sw}(\theta_m)|^{\frac{4}{\alpha}}, \\ &|G_{sw}(\theta_m)| = min\{|G^{(1)}(\theta_m)|, |G^{(2)}(\theta_m)|\}, \\ &\theta_m = m\Delta. \end{aligned} \tag{17}$$

We model the problem of optimal artificial fading as a problem of minimizing the predicted unnecessary coverage area expressed in (17) under double-beam switching transmission. This problem is a nonlinear programming problem with the complex antenna array weight vectors $\mathbf{w}^{(1)}$ and $\mathbf{w}^{(2)}$ as optimization variables. Without loss of generality, we normalize the antenna array directional gain with respect to $G^{(n)}(0) = 1$. Since $\frac{\pi}{M}\left(\frac{P_0}{R_{th}PL_0}\right)^{\frac{2}{\alpha}}$ is a constant, we can remove it from the objective function without affecting the optimal solution, and get the problem formulation below:

$$\begin{aligned} \min_{\mathbf{w^{(1)}},\mathbf{w^{(2)}}} \quad & \sum_{m=l}^{M-1-l} |G_{sw}(\theta_m)|^{\frac{4}{\alpha}} \\ \text{s. t.} \quad & |G_{sw}(\theta_m)| = min\{|G^{(1)}(\theta_m)|, |G^{(2)}(\theta_m)|\} \\ & G^{(n)}(0) = 1,\ n = 1, 2 \\ & l = \lfloor \tfrac{BW}{2\Delta} \rfloor. \end{aligned} \tag{18}$$

The problem in (18) is non-convex and it is generally impossible to directly solve it and get a rigorous optimal solution. So we need to seek approximation algorithms based on the practical properties of smart antenna beamforming. As shown in formulation (18), in a specific direction, only the smaller directional gain between the two beamforming patterns contributes to the objective function, and hence, needs to be minimized. Therefore, a good solution set to (18) is to divide the whole range of undesired transmit directions into two sets. Each beamforming pattern is tuned only to minimize the coverage area within one set while having freedom to transmit larger power on the other set. In other words, one pattern's minimized direction set is always overlapped with the other pattern's non-minimized direction set, except the direction towards the receiver, where main beams of the two pattern are overlapped. The pattern pair in Fig. 2 also shows this idea. To determine the allocation of direction sets to be minimized for each pattern for the above type of solutions, note that, from the aspect of antenna pattern synthesis, for an antenna array with N elements, at most $N-1$ nulls can be formed according to the the antenna array's degree of freedom [15]. Also, it has been shown that by combining multiple nulls (placing them closely), a wider or deeper total null space can be formed [15] [16]. Hence, this indicates that we should combine multiple nulls of a single synthesized pattern to form a wide null which covers a relatively large phase range. Thus, we divide the range of undesired transmit directions into two continuous sectors with equivalent size. We let each beamforming pattern form a wide null in one sector by tuning the complex weight vectors. Thus, along every undesired transmit direction, the transmitted signal is nulled out at least in every other pattern switching period, which is exactly how artificial fading works. Then, the problem is reformulated as the following convex optimization problem which can be directly solved using existing nonlinear optimization software such like cvx [17].

$$\begin{aligned} \min_{\mathbf{w^{(1)}},\mathbf{w^{(2)}}} \quad & \sum_{m=l}^{\lfloor \frac{M-1}{2} \rfloor} |G^{(1)}(\theta_m)|^{\frac{4}{\alpha}} + \sum_{m=\lceil \frac{M-1}{2} \rceil}^{M-1-l} |G^{(2)}(\theta_m)|^{\frac{4}{\alpha}} \\ \text{s. t.} \quad & G^{(n)}(0) = 1,\ n = 1, 2 \\ & \theta_m = m\Delta \end{aligned} \tag{19}$$

D. Limited total transmit power

Taking into account the potential transmit power restriction to the artificial fading scheme, the total transmit power P_{sw}

can be expressed as:

$$P_{sw} = \frac{P_0}{2M} \sum_{m=0}^{M-1} |G^{(1)}(\theta_m)|^2 + |G^{(2)}(\theta_m)|^2. \quad (20)$$

Suppose the transmit power limit is P_{th}. By combining this constraint into the double-beam optimization problem in (19), we get the form of our artificial fading optimization problem under limited total transmit power:

$$\begin{aligned} \min_{\mathbf{w^{(1)}},\mathbf{w^{(2)}}} \quad & \sum_{m=l}^{\lfloor \frac{M-1}{2} \rfloor} |G^{(1)}(\theta_m)|^{\frac{4}{\alpha}} + \sum_{m=\lfloor \frac{M-1}{2} \rfloor}^{M-1-l} |G^{(2)}(\theta_m)|^{\frac{4}{\alpha}} \\ \text{s. t.} \quad & G^{(n)}(0) = 1, \ n = 1, 2 \\ & \sum_{m=0}^{M-1} |G^{(1)}(\theta_m)|^2 + |G^{(2)}(\theta_m)|^2 \leq \frac{2MP_{th}}{P_0} \\ & \theta_m = m\Delta. \end{aligned} \quad (21)$$

V. Simulation Evaluation

To evaluate the performance of the proposed artificial fading scheme in reducing the unnecessary coverage area, we optimize the double-pattern synthesis by solving problems (19) and (21), and simulate the signal propagation under artificial fading in Matlab environment. We first show an example of the optimized pattern pair and compare the performance with single pattern beamforming using log-distance path loss model. Then we employ Monte Carlo simulation to compare the reduced unnecessary coverage areas using single pattern beamforming and the proposed artificial fading scheme with the presence of shadow fading and multipath Rayleigh fading.

The setting of the parameters is as below. The path loss exponent is $\alpha = 3.5$. Radio sensitivity is R_{th}(dBm) $= -70$ dBm. The required transmit power, when omni directional antenna is used, is P_0(dBm) $= 10$ dBm and the path loss at $d_0 = 1m$ is PL_0(dB) =30 dB.

A. Example of optimized beamforming pattern pair

Fig. 4(a) illustrates a simple example of the optimized beamforming pattern pair for maximizing the effect of artificial fading. In this case, we assume that the receiver is in the direction of $\theta = 0°$. The smart antenna array consists of $N_{ant} = 6$ omni antenna elements and the width of the required main beam towards the receiver is $BW = 30°$. As shown in Fig. 4(a), pattern 1 and pattern 2 both have a wide main lobe, which contains the direction of the receiver, and a wide null that spans a separate direction sector. Thus, in the undesired directions, at least one pattern can null out the transmitted signal during its operation period. While in the direction to the intended receiver, the antenna has a constant high gain. As a comparison, the optimal radiation pattern using single-pattern beamforming is shown in Fig. 4(b), which is also synthesized by the smart antenna array with $N_{ant} = 6$ elements. Although this pattern has already been optimized to minimize the unnecessary coverage area, it still has considerable side lobes which result in unnecessary coverage. Differently, the overlapped pattern in Fig. 4(a) has much smaller side lobes, due to the cooperation between the two patterns. As a result, the predicted effective coverage area of double-beam switching has a much smaller unnecessary portion compared with single beamforming pattern as shown in Fig. 4(c).

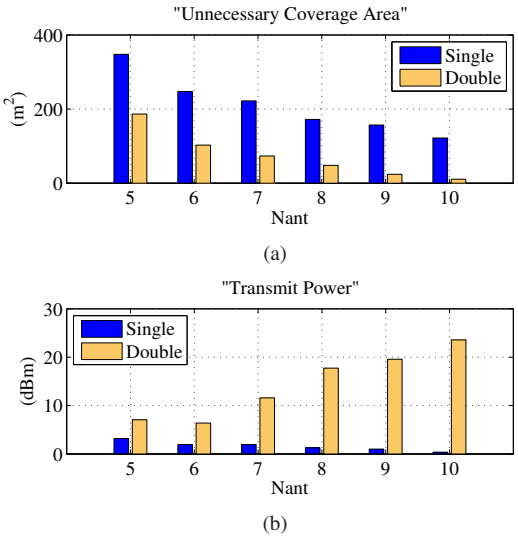

Fig. 5. Performance comparison without transmit power limit.

B. Analysis in ideal channel

In this part, we analyze the performance of the proposed artificial fading scheme and single pattern beamforming scheme using log-distance path loss model by changing the number of antenna elements (N_{ant}) and the total transmit power constraint (P_{th}).

Fig. 5(a) illustrates the minimized unnecessary coverage area of single-pattern beamforming and double-beam switching. The double-beam patterns are generated from the formulation in (19). Transmit power constraint is not considered yet in order to find the best capability of artificial fading scheme in trading power consumption for enhancing anti-eavesdropping. It is indicated in the figure that as N_{ant} increases, the minimum unnecessary coverage area decreases under both schemes. This is because the smart antenna array with more antenna elements has more flexibility in tuning the radiation pattern. Comparatively, for a given number of antenna elements, double-beam switching transmission can reduce more than half the unnecessary coverage area of single pattern beamforming.

We also compare the power consumption under the two schemes in Fig. 5(b). We discover that for single pattern beamforming, as N_{ant} increases, the total transmit power for achieving the minimum unnecessary coverage is decreasing. The reason is that for single patten beamforming, the main strategy for anti-eavesdropping is reducing the transmit power in undesired directions. However, the proposed artificial fading scheme, realized by double-beam switching, reduces the unnecessary coverage area by corrupting wireless signals in undesired directions. Thus it will trade power consumption for further reduction of unnecessary coverage area whenever it is

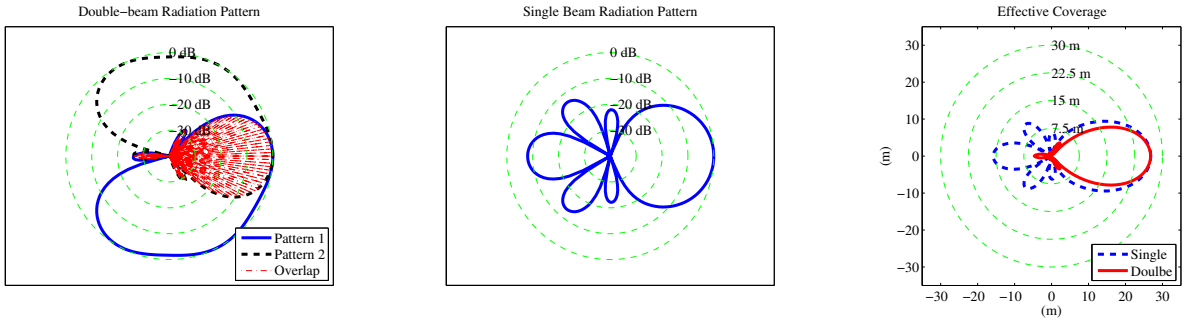

(a) (b) (c)

Fig. 4. Radiation patterns and predicted effective coverage of single beamforming pattern and double-beam switching.

possible. Therefore, we can observe in Fig. 5(b) that the total transmit power consumed by double-beam switching is higher than single pattern beamforming. This observation implies that the performance of the proposed artificial fading scheme is related to the allowed total transmit power.

To analyze how the performance of the artificial fading scheme is related to the total transmit power limit, we set $N_{ant} = 6$ and $BW = 30°$. The constraint on max total transmit power is added to the optimization problem defined in (21). The result is shown in Fig. 6. The horizontal coordinate represents the upper bound constraint of the transmit power for the artificial fading scheme and the vertical coordinate shows the minimum unnecessary coverage area using optimized beamforming pattern pair. Generally, the minimum unnecessary coverage area decreases when allowed transmit power increases. However, when the transmit power limit reaches a certain value, (4.2 mW in this example), the minimum unnecessary coverage area cannot be further reduced, because the artificial fading scheme already reaches its optimum under this antenna array geometry.

In order to compare the performance of the single pattern beamforming scheme and the proposed artificial fading scheme under a practical transmit power constraint, we assume that the transmit power limit in problem (21) is P_{th} =10mW, which equals the required transmit power when omni directional antenna is used, and run simulations with different value of N_{ant} and BW. The minimized unnecessary coverage area under different parameter settings is illustrated in Fig. 7(a) and Fig. 7(b). We can see that the artificial fading scheme significantly outperforms the single pattern beamforming scheme when its power consumption is no more than the transmit power consumed by an omni directional antenna.

C. Evaluation in shadow fading channel

In this part, we evaluate the performance of the proposed artificial fading scheme under shadow fading. We assume that the standard deviation of the log normal shadow fading is $\sigma = 5$ (dB). For each parameter setting, 1000 beam switching periods are simulated.

First, with the same parameter settings as the case in Section V-A, Fig. 8(a) and Fig. 8(b) show the outage probabilities (P_{out}) of single pattern beamforming and double-beam switching under shadow fading in a $80 * 80$ m^2 area, respectively. Each color represents a level of P_{out} as shown on the right side of the figure. For both schemes, we set $N_{ant} = 6$ and $BW = 30°$. Following the example of IEEE 802.11 discussed in Section III-B, because signal outage with probability larger than 0.4 is beyond the capability of the error correction code, the effective coverage region should be inside the area with $P_{out} \leq 0.4$. Since we assume that the intended receiver is in the $0°$ direction, the covered regions of both single- and double-beamforming schemes according to $P_{out} \leq 0.4$ point to the right side. We find that for $P_{out} \leq 0.4$, the covered region in Fig. 8(a) is almost without side lobes, and is apparently smaller than the covered region in Fig. 8(b). This is consistent with the result in Fig. 4(c) which is obtained under idea channel condition. The only difference is that due to the shadow fading and the outage tolerance capability of the error correction code, the real effective coverage area might differ from the value in ideal communication environments. However, the shape of the effective coverage area is still roughly the same with the predicted effective coverage in ideal channel. Also, as shown in Fig. 8(c), the curve segments from $P_{out} = 0$ to $P_{out} = 0.4$ implie that the proposed artificial fading scheme creates smaller unnecessary coverage area than single pattern beamforming scheme. Although for $P_{out} > 0.5$, double-beam switching transmission has larger covered area, within the regions where signal outage probability is larger than 0.5, the eavesdropper in those regions cannot successfully decode the signal and there is no information leakage concern.

Next, we change the value of N_{ant} and simulate the performance of the proposed artificial fading scheme with different total transmit power limits (P_{th}). The unnecessary coverage area using single pattern beamforming is listed in Table I as reference. The performance of the artificial fading scheme is provided in Table II. By comparing the two tables, we can see that the proposed artificial fading scheme can achieve greater reduction of unnecessary coverage area against the single pattern beamforming scheme in shadow fading environment and its performance tends to improve when higer transmit power consumption is allowed.

D. Evaluation in multipath Rayleigh fading channel

This part shows the simulation results under multipath Rayleigh fading. For the same values of N_{ant} and BW, the spacial distribution of outage probability under Rayleigh

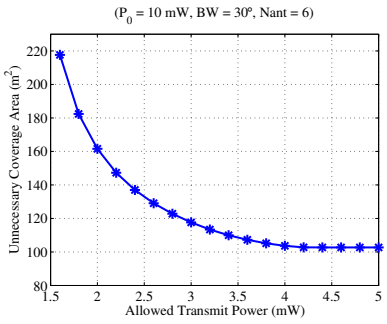

Fig. 6. Minimum unnecessary coverage area v.s. transmit power limit.

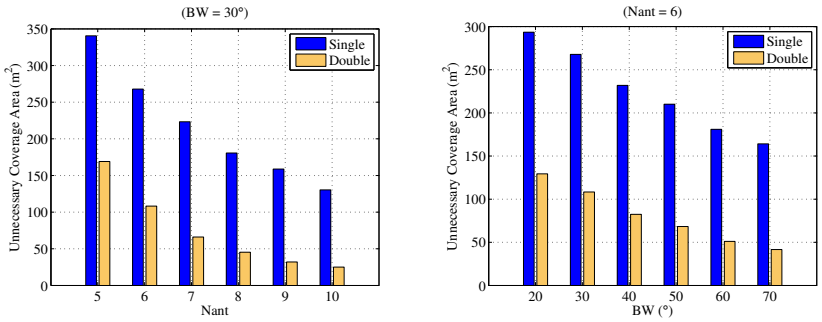

(a) (b)

Fig. 7. Performance comparison under transmit power limit defined by the required transmit power when omni-directional antenna is used (10 mW).

TABLE I
UNNECESSARY COVERAGE AREA OF SINGLE PATTERN BEAMFORMING UNDER **SHADOW FADING**. (m^2)

P_{out}	N_{ant} = 6	N_{ant} = 8	N_{ant} = 10
0.1	336	242	181
0.2	443	315	244
0.3	555	394	303
0.4	664	477	372

TABLE II
UNNECESSARY COVERAGE AREA OF DOUBLE-BEAM SWITCHING UNDER **SHADOW FADING**. (m^2)

P_{th} (mW)	P_{out}	N_{ant} = 6	N_{ant} = 8	N_{ant} = 10
2	0.1	308	193	136
	0.2	420	279	197
	0.3	531	354	264
	0.4	653	466	356
6	0.1	200	150	108
	0.2	284	219	151
	0.3	374	298	213
	0.4	501	409	295
10	0.1	229	143	95
	0.2	321	217	150
	0.3	426	288	204
	0.4	545	415	287

TABLE III
UNNECESSARY COVERAGE AREA OF SINGLE PATTERN BEAMFORMING UNDER **MULTIPATH RAYLEIGH FADING**. (m^2)

P_{out}	N_{ant} = 6	N_{ant} = 8	N_{ant} = 10
0.1	152	116	90
0.2	250	184	149
0.3	343	256	199
0.4	448	334	262

fading has the same shape and trend with the results under shadow fading, which are shown in Fig. 8, even though the exact size of each region corresponding to a given outage probability might be slightly different. Thus, we omit the figure of spacial outage probability distribution for Rayleigh fading channel due to space limitations. Table III and Table IV list the unnecessary coverage under multipath Rayleigh fading for the single pattern beamforming scheme and the artificial fading scheme, respectively. Again, P_{th} is the upper limit of total transmit power consumption applied to the double-beam optimization problem in (21). Consistently with the conclusion in Section V-C, results in the two tables show that the proposed artificial fading scheme can achieve greater reduction of unnecessary coverage area against the single pattern beamforming scheme in Rayleigh fading environment. Meanwhile, the tradeoff between the reduction on the unnecessary coverage and the total power consumption also exists in Rayleigh fading environment.

VI. Discussion

A. Node mobility

In this work, we assume that the direction of the intended receiver is known to the transmitter that is using artificial fading scheme. However, this does not necessarily mean that both the transmitter and the intended receiver must be static. Remember that in the artificial fading scheme, the transmitter is equipped with a smart antenna array. The smart antenna array enables the transmitter to track the Direction of Arrival (DOA) of the signal from the reverse link, and hence, get the direction of the mobile receiver. Direction finding using antenna array is a well studied area and lots of algorithms are available [18]–[21]. Since DOA estimation is out of the scope of this paper, we simply assume that the transmitter with a smart antenna array can use state of the art DOA estimation algorithms to find the direction of a mobile receiver.

B. Collaborative eavesdropping attack

It is possible for the eavesdroppers in multiple locations to collaboratively exchange and merge their received signal fragments. However, precise synchronization among the eavesdroppers is required to correctly merge the signal fragments, which dramatically increases the cost for eavesdropping. Even collaboration is possible, a simple addition of an extra antenna array to our artificial fading scheme can defeat such collaboration effort. The transmitter can use the additional antenna array to transmit noise signal using a carefully crafted pattern, which fills the null directions of one beamforming pattern with noise and blurs the timing of beam pattern switching. In this way, it is difficult for eavesdroppers to differentiate and merge their received useful information signals.

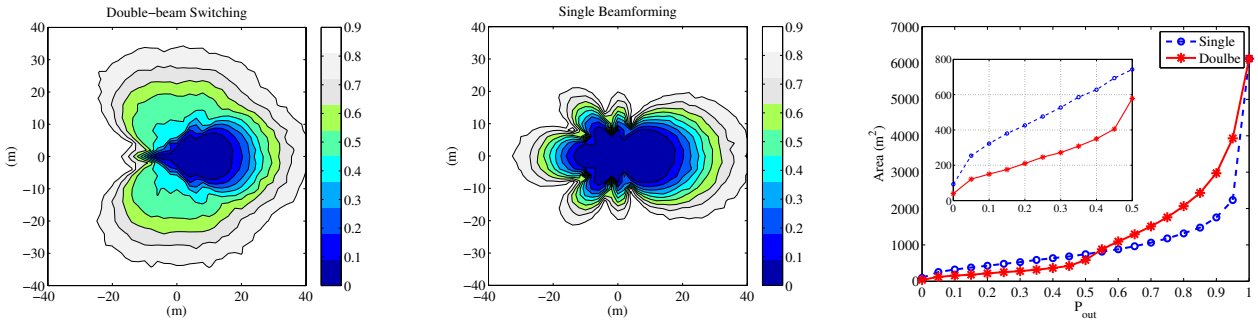

(a) (b) (c)

Fig. 8. Outage Probability under single pattern beamforming and double-beam switching in shadow fading channel.

TABLE IV
UNNECESSARY COVERAGE AREA OF DOUBLE-BEAM SWITCHING UNDER **MULTIPATH RAYLEIGH FADING**. (m^2)

P_{th}(mW)	P_{out}	N_{ant} = 6	N_{ant} = 8	N_{ant} = 10
2	0.1	128	102	70
	0.2	215	168	128
	0.3	303	247	182
	0.4	414	334	256
6	0.1	105	81	58
	0.2	178	145	106
	0.3	259	214	163
	0.4	374	311	236
10	0.1	104	69	39
	0.2	179	127	67
	0.3	262	196	104
	0.4	373	295	163

VII. CONCLUSION

The broadcast nature of wireless communication networks makes the communicated confidential information at the risk of being eavesdropped. We propose a physical layer anti-eavesdropping scheme using the novel concept of artificial fading, which is realized by double-beam switching of smart antenna array. Our scheme optimizes the switched beamforming pattern pair, such that the wireless communication links in undesired directions are unusable because of the intentionally produced artificial fading, while the intended transmit direction gets persistent good signal quality. In this way, the unnecessary coverage area is significantly reduced and the secrecy measure is improved. Simulation results show that our artificial fading scheme outperforms single pattern beamforming scheme in reducing unnecessary coverage and provides a controllable tradeoff between the total transmit power consumption and the reduction of unnecessary coverage area.

ACKNOWLEDGMENT

This work is supported by National Science Foundation fund number ECCS-0802112 and the Institute for Critical Technology and Applied Science (ICTAS).

REFERENCES

[1] A. Mukherjee, S. A. Fakoorian, J. Huang, and A. L. Swindlehurst, "Principles of physical layer security in multiuser wireless networks: A survey," 2010. [Online]. Available: http://arxiv.org/abs/1011.3754

[2] X. Li, M. Chen, and E. Ratazzi, "Array-transmission based physical-layer security techniques for wireless sensor networks," in *IEEE Int. Conf. on Mechatronics and Automation*, 2005.

[3] X. Li, J. Hwu, and E. P. Ratazzi, "Using antenna array redundancy and channel diversity for secure wireless transmissions," *Journal of Communications*, vol. 2, no. 3, pp. 24–32, 2007.

[4] S. Goel and R. Negi, "Guaranteeing secrecy using artificial noise," *IEEE Transactions on Wireless Communications*, vol. 7, no. 6, pp. 2180–2189, 2008.

[5] X. Zhou and M. McKay, "Secure transmission with artificial noise over fading channels: Achievable rate and optimal power allocation," *IEEE Transactions on Vehicular Technology*, vol. 59, no. 8, pp. 3831–3842, 2010.

[6] J. Carey and D. Grunwald, "Enhancing WLAN security with smart antennas: a physical layer response for information assurance," in *IEEE Vehicular Technology Conference*, 2004.

[7] S. Lakshmanan, C. Tsao, and R. Sivakumar, "Aegis: Physical space security for wireless networks with smart antennas," *IEEE/ACM Transactions on Networking*, vol. 18, no. 4, pp. 1105–1118, 2010.

[8] F. Gross, *Smart Antennas for Wireless Communications: With MATLAB*. McGraw-Hill, 2005.

[9] A. A. Sani, L. Zhong, and A. Sabharwal, "Directional antenna diversity for mobile devices: Characterizations and solutions," in *Proceedings of ACM MobiCom*, 2010.

[10] H. Yu, L. Zhong, A. Sabharwal, and D. Kao, "Beamforming on mobile devices: A first study," in *Proceedings of ACM MobiCom*, 2011.

[11] Plasma Antennas Limited, "Selectable Multibeam Antennas," Jul 2011. [Online]. Available: http://www.plasmaantennas.com

[12] J. Proakis, *Digital Communications*, 4th ed. McGraw-Hill, 2001.

[13] "Part 11: Wireless LAN medium access control (MAC) and physical layer (PHY) specifications," *IEEE Std 802.11-2007*.

[14] R. Vescovo, "Pattern synthesis with null constraints for circular arrays of equally spaced isotropic elements," in *IEE Proceedings of Microwaves, Antennas and Propagation*, vol. 143, no. 2, 1996, pp. 103–106.

[15] R. Mailloux, *Phased array antenna handbook*. Artech House, 2005.

[16] H. Steyskal, "Wide-band nulling performance versus number of pattern constraints for an array antenna," *IEEE Transactions on Antennas and Propagation*, vol. 31, no. 1, pp. 159–163, 1983.

[17] M. Grant and S. Boyd, "CVX: Matlab software for disciplined convex programming, version 1.21," http://cvxr.com/cvx, Apr. 2011.

[18] R. Schmidt, "Multiple emitter location and signal parameter estimation," *IEEE Transactions on Antennas and Propagation*, vol. 34, no. 3, pp. 276–280, Mar 1986.

[19] R. Roy and T. Kailath, "Esprit-estimation of signal parameters via rotational invariance techniques," *IEEE Transactions on Acoustics Speech and Signal Processing,*, vol. 37, no. 7, pp. 984–995, Jul. 1989.

[20] R. Goossens and H. Rogier, "A hybrid UCA-RARE/Root-MUSIC approach for 2-D direction of arrival estimation in uniform circular arrays in the presence of mutual coupling," *IEEE Transactions on Antennas and Propagation*, vol. 55, no. 3, pp. 841–849, Mar. 2007.

[21] Y. H. Ko, Y. J. Kim, H. I. Yoo, W. Y. Yang, and Y. S. Cho, "2-D DoA estimation with cell searching for a mobile relay station with uniform circular array," *IEEE Transactions on Communications*, vol. 58, no. 10, pp. 2805–2809, Oct. 2010.